2024 Asia Pacific Conference on Innovation in Technology (APCIT)
Mysuru, India. Jul 26-27, 2024

2024 Asia Pacific Conference on Innovation in Technology (APCIT) | 979-8-3503-6153-7/24/$31.00 ©2024 IEEE | DOI: 10.1109/APCIT62007.2024.10673586

LaCK: *L*ung C*a*ncer *C*lassification and Detection using Convolutional Neural Network-based Gated Recurrent Unit Neural Networ*k* Model

Machakanti Navya Thara
Artificial Intelligence & Machine Learning
Nalla Malla Reddy Engineering College
Hyderabad, India
machakantinavyathara333@gmail.com

Kalyan Chatterjee
Computer Science & Engineering
Nalla Malla Reddy Engineering College
Hyderabad, India
kalyanchatterjee.cse@nmrec.edu.in

Muntha Raju
Computer Science & Engineering
Nalla Malla Reddy Engineering College
Hyderabad, India
raju.cse@nmrec.edu.in

Sandip Rout
Mathematics
Government Autonomous College
Angul, Odisha Dept. of Higher Education,
Government of Odisha, India
sandiprout7@gmail.com

M. Priyadharshini
Computer Science & Engineering
Nalla Malla Reddy Engineering College
Hyderabad, India
priyadharshini.cse@nmrec.edu.in

Kokkula Shiva Prasad
Computer Science & Engineering
Nalla Malla Reddy Engineering College
Hyderabad, India
shivaprasad.ece@nmrec.edu.in

Samala Suraj Kumar
Artificial Intelligence & Machine Learning
Nalla Malla Reddy Engineering College
Hyderabad, India
samalasuraj@gmail.com

Mandadi Sriya Reddy
Artificial Intelligence & Machine Learning
Nalla Malla Reddy Engineering College
Hyderabad, India
20b61a6629@nmrec.edu.in

***Abstract*—Cancer instills fear in people worldwide, with millions succumbing to its grasp each year. Among the various types, lung cancer stands as a prominent contributor to this alarming statistic. Therefore, this novel research *L*ung C*a*ncer *C*lassification and Detection using Convolutional Neural Network-based Gated Recurrent Unit Neural Networ*k* Model (LaCK) has focused on classifying lung cancer, notably Non-Small Cell Lung Cancer, which constitutes the majority of cases. We employed five units of gated recurrent unit neural network (GRU-NN) together to achieve this classification, utilizing logistic regression (LR) and support vector classifier (SVC) models for comparisons. Among all models, the LaCK model demonstrated remarkable accuracy, achieving approximately 98% success rate, outperforming its counterparts. Implementing this model in clinical settings enables medical professionals to establish a precise and automated approach to diagnosing lung cancer.**

***Index Terms*—Classification, Detection, Deep Learning (DL), Lung Cancer, Machine Learning (ML), Non-Small Cell.**

I. Introduction

The lung, a vital organ facilitating breathing, becomes susceptible to the formation of lumps or tumors when cells undergo uncontrolled growth due to inactive cancer-suppressor genes. These growths, called tumors, can be benign or malignant. Malignant tumors, recognized as cancer, exhibit heightened aggressiveness, metastasis, and the ability to spread throughout the body. Symptoms of lung cancer include difficulty breathing, bloody cough, weight loss, etc. Certain chemicals like arsenic, nickel, and silica elevate the risk.

Lung cancer is categorized into three types: non-small cell, small cell, and carcinoid. Among these, the small cell type is particularly aggressive, rapidly growing and spreading throughout the body. Inorganic materials like asbestos, nickel, chromium, and organic substances such as benzene and benzopyrene can enter the lungs through the air, contributing to lung cancer. Persistent harm to the lungs is a crucial factor.

Tobacco use accounts for 85% of lung cancer cases, while the remaining 10%-15% affect non-smokers. Globally, lung cancer stands as a leading cause of illness and death in males, with women ranking second in fatalities. Annually, 1.3 million people succumb to lung cancer.

The primary contributions of this study are detailed as follows:

- This work introduces an innovative LaCK model to enhance the classification and detection of lung cancer by synergizing the capabilities of deep convolutional neural networks (DCNNs) with GRUs.
- Another noteworthy contribution lies in the reduced training time achieved by incorporating the five units of GRUs with five units of DCNNs, which enhances the capacity to identify the lung abnormalities of the LaCK model.

II. Related Work

Bhatia et al. [1] used the deep learning models by employing Tree-based classifiers like XGBoost and Random Forest.

Their ensemble approach, combining UNet+RandomForest and ResNet+XGBoost, yielded an accuracy of 84%, surpassing the individual accuracies of UNet (74%) and ResNet (75.98%).

Kriegsmann et al. [2] investigated various CNN models for detecting four cancer subtypes, concluding that an optimized architecture based on InceptionV3 CNN yielded the most precise outcomes.

Lei Cong et al. [3] discussed the importance of recognizing and understanding malignant cell features for diagnosing and treating primary or metastatic malignancies in lung cancer research.

Intense deep learning (DL) techniques [4], [5] have revolutionized biomedical applications, allowing machines to handle large-scale datasets. Earlier studies often focused on DL for image classification, with some concentrating on colon cancer while others prioritized lung cancer.

Kumar et al. [6] highlighted the superior properties of DenseNet-121 in capturing meaningful features compared to other pre-trained convolutional neural networks.

Hlavcheva [7] used convolutional neural networks (CNNs) to assess medical photos to classify colon and lung cancer, achieving an accuracy of 94.6%.

Sun et al. [8] developed an ML-based model to determine malignancy in lung nodules using deep structured algorithms, achieving an accuracy of 87.14% with SDAE, DBN, and CNN.

Filho et al. [9] applied image segmentation to preprocess CT images depicting lung nodules, resulting in a 92.6% accuracy in the differentiation between benign and malignant tumors.

Masood et al. [10] introduced the DFCNet model, based on a deep CNN, for classifying CT scan pictures of pulmonary nodules, achieving an accuracy of 84.5%.

Urban et al. [11] created deep CNNs for polyp detection in colonoscopies, achieving an accuracy of 96.4%.

Suresh and Mohan [12] proposed an eight-layer CNN architecture for classifying lung lesions in CT scan images, achieving 93.9% accuracy for classification.

Masud et al. [13] introduced a straightforward deep-learning method featuring a CNN architecture comprising four convolutional layers, achieving an accuracy rate of 97.9%.

III. System Architecture & Problem Formulation

A. System Architecture

The system architecture for the LaCK model can be outlined as follows:

1) **Input Layer:** Input layer contains various input features like gender, age, smoking history, presence of yellow fingers, anxiety, peer pressure, chronic disease, fatigue, allergy, wheezing, alcohol consumption, coughing, shortness of breath, swallowing difficulty, and chest pain.
2) **Preprocessing:** Data preprocessing involves normalization, scaling, and handling missing values to ensure uniformity and enhance model performance.
3) **Embedding Layer:** For categorical features like gender, an embedding layer converts them into a numerical format suitable for input into the neural network.
4) **Sequential GRU Layers:** The core of the architecture consists of sequential GRU layers. GRUs are a type of recurrent neural network (RNN) that excels at capturing sequential dependencies in data. These layers analyze the temporal relationships among the input features.
5) **Dense Layers:** Dense layers are incorporated for feature abstraction and extraction following the GRU layers. These layers facilitate the transformation of the learned features into a format suitable for classification.
6) **Output Layer:** The output layer is designed for binary classification, predicting whether the patient has lung cancer (YES) or not (NO).
7) **Activation Function:** An appropriate activation function, such as sigmoid, is utilized in the output layer to produce probabilities for the binary classification.
8) **Loss Function and Optimizer:** Mean Square Errror (MSE) and Adam are the loss function and an optimizer, respectively.
9) **Training:** The LaCK model is trained on the provided dataset, adjusting weights and biases to minimize the loss function during training.
10) **Evaluation:** The LaCK model is evaluated on a separate validation dataset to assess its accuracy.
11) **Inference:** Once trained, the LaCK model can be utilized for making predictions on new data, providing insights into the likelihood of an individual having lung cancer based on the input features.
12) **Post-processing:** If necessary, the final output can undergo post-processing steps to enhance interpretability.

Therefore, utilizing a GRU Neural Network in this architecture allows for effective modeling of temporal dependencies within the input features, making it well-suited for tasks involving sequential data, such as the prediction of lung cancer based on various patient attributes described in Figure 1.

B. Problem Formulation

Let X be the set of input features representing patient attributes, and Y be the binary output indicating the presence ($Y = 1$) or absence ($Y = 0$) of lung cancer.

The input features are defined as follows: X=gender, age, smoking, yellow fingers, anxiety, peer pressure, chronic disease, fatigue, allergy, wheezing, alcohol, coughing, shortness of breath, swallowing difficulty, chest pain

The task is to train a GRU Neural Network to learn a mapping $f : X \rightarrow Y$, such that the model can classify whether a patient has lung cancer or not.

The model parameters are denoted as θ, and the output of the GRU network is $\hat{Y}$, representing the predicted probability of lung cancer.

The training process involves minimizing the binary cross-entropy loss $J(\theta)$ over a dataset of labeled examples $\{(X^{(i)}, Y^{(i)})\}$:

$$J(\theta) = -\frac{1}{N}\sum_{i=1}^{N}\left[Y^{(i)}\log(\hat{Y}^{(i)}) + (1 - Y^{(i)})\log(1 - \hat{Y}^{(i)})\right]$$

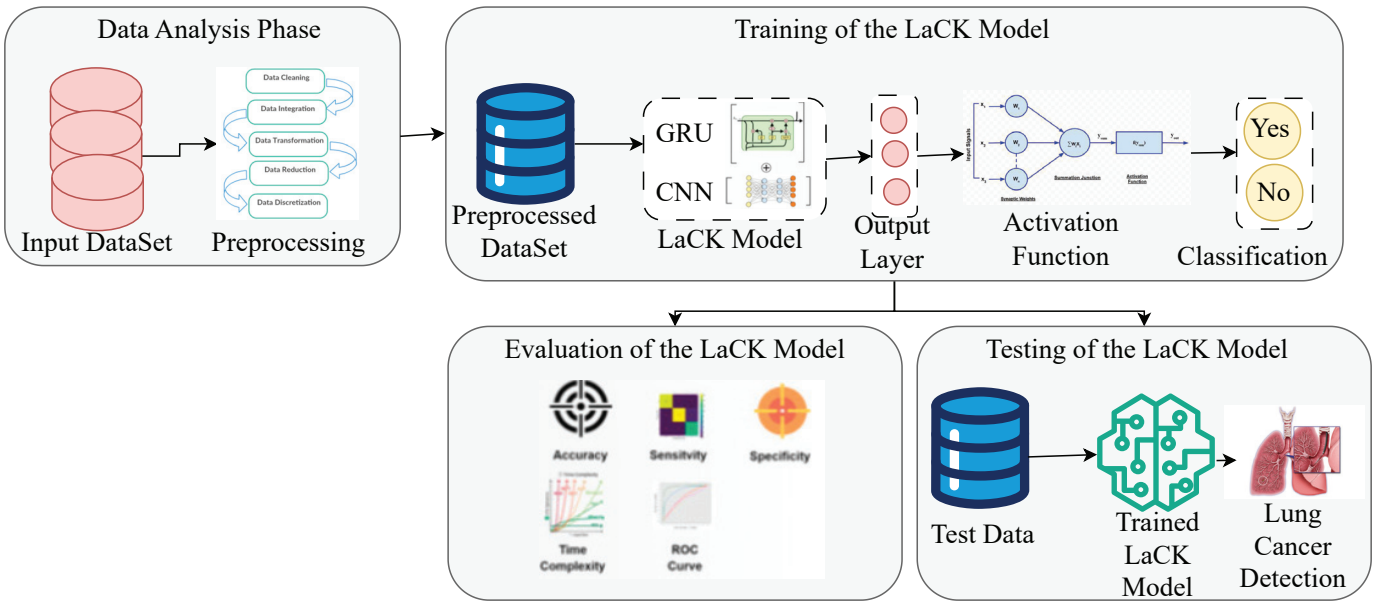

Fig. 1. System Architecture of the LaCK Model.

Here, N is the total number of instances in the dataset. The model parameters θ are updated during training using an optimization algorithm, such as Adam.

IV. Dataset

The efficiency of the cancer prediction system enables individuals to ascertain their cancer risk at a low cost, facilitating informed decision-making based on their cancer risk status. The data originates from the online lung cancer prediction system's website (Kaggle) [14], encompassing a total of 16 attributes and 284 instances.

V. Proposed Model

The LaCK model, illustrated in Figure 2, presents an innovative approach to lung cancer analysis. It comprises four fundamental components: i) input layer, ii) feature extraction layer, iii) output layer, and iv) classification layer.

The input layer receives input data, which is processed by a deep convolutional neural network (DCNN) within the feature extraction layer. The output layer then provides the extracted features. Ultimately, lung cancer is classified and detected through the classification layer.

The feature extraction layer of the DCNN contains five units of convolutional layers (Conv) and pooling layers (Pool), respectively, because of the efficiency of the LaCK model as described in Table I. Convolutional layers are crucial in extracting local features from the used dataset [14]. Each convolutional layer adeptly captures spatial patterns for identifying lung abnormalities and employs a set of weighted kernels W_l for layer l to extract local features x_{l-1} from the input. The following equation represents this process:

$$C_l = W_l^T X_{l-1} + b_l \tag{1}$$

TABLE I
Feature Extraction Layer of DCNN

Layer	Operation	Output Size
Conv1	Convolutional	$H_1 \times W_1 \times C_1$
Pool1	Max Pooling	$H_2 \times W_2 \times C_1$
Conv2	Convolutional	$H_3 \times W_3 \times C_2$
Pool2	Max Pooling	$H_4 \times W_4 \times C_2$
Conv3	Convolutional	$H_5 \times W_5 \times C_3$
Pool3	Max Pooling	$H_6 \times W_6 \times C_3$
Conv4	Convolutional	$H_7 \times W_7 \times C_4$
Pool4	Max Pooling	$H_8 \times W_8 \times C_4$
Conv5	Convolutional	$H_9 \times W_9 \times C_5$
Pool5	Max Pooling	$H_{10} \times W_{10} \times C_5$

TABLE II
Computational Matrices for Five Units of GRUs

GRU Unit	Computational Matrices
GRU1	$\begin{bmatrix} W_{xr} & W_{xu} \\ W_{hr} & W_{hu} \end{bmatrix}, \begin{bmatrix} b_r \\ b_u \end{bmatrix}$
GRU2	$\begin{bmatrix} W_{xr} & W_{xu} \\ W_{hr} & W_{hu} \end{bmatrix}, \begin{bmatrix} b_r \\ b_u \end{bmatrix}$
GRU3	$\begin{bmatrix} W_{xr} & W_{xu} \\ W_{hr} & W_{hu} \end{bmatrix}, \begin{bmatrix} b_r \\ b_u \end{bmatrix}$
GRU4	$\begin{bmatrix} W_{xr} & W_{xu} \\ W_{hr} & W_{hu} \end{bmatrix}, \begin{bmatrix} b_r \\ b_u \end{bmatrix}$
GRU5	$\begin{bmatrix} W_{xr} & W_{xu} \\ W_{hr} & W_{hu} \end{bmatrix}, \begin{bmatrix} b_r \\ b_u \end{bmatrix}$

In the final stage of the LaCK model, five units of GRUs are utilized for classification purposes as described in Table II. The features extracted by the DCNN undergo conversion into 1D vectors via a flatten layer. These resultant feature vectors are then fed into the GRU layer. These GRU layers are responsible for handling the sequential data and effectively capture temporal dependencies among the features. The GRU layer comprises two key components: the update gate (z_t) and

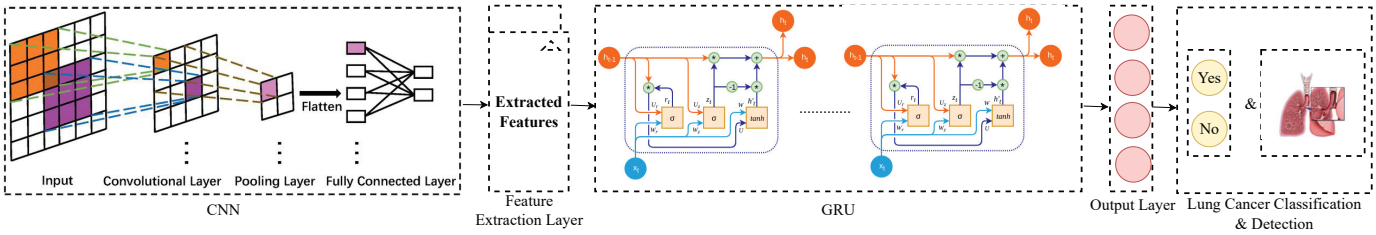

Fig. 2. Proposed Lack Model.

the reset gate (r_t). These gates play a crucial role in regulating the information flow within the GRU, facilitating the capture of pertinent temporal patterns. The following equations can represent the computations of the GRU layer:

$$z_t = \sigma(W_z \cdot [h_{t-1}, x_t] + b_z)$$
$$r_t = \sigma(W_r \cdot [h_{t-1}, x_t] + b_r)$$
$$\tilde{h}_t = \tanh(W \cdot [r_t \odot h_{t-1}, x_t] + b)$$
$$h_t = (1 - z_t) \odot h_{t-1} + z_t \odot \tilde{h}_t$$

Moreover, by integrating CNN with GRU to formulate the LaCK model, the strengths of both architectures are effectively combined, thereby mitigating the influence of noise on individual predictions.

Algorithm 1 describes the proposed LaCK model.

Algorithm 1 Lung Cancer Classification and Detection using CNN and GRU based LaCK Model

Input: Lung cancer dataset $\mathcal{D}$ [14], CNN filters F, GRU neurons N, etc.
Output: Predicted lung cancer labels
Begin
Preprocess The lung cancer dataset $\mathcal{D}$ [14]
Initialize CNN filters F and GRU neurons N
Define CNN Architecture with convolutional layers for spatial feature extraction

$$C_l = \sigma(W_l^T X_{l-1} + b_l)$$

Define GRU Architecture for capturing temporal dependencies

$$z_t = \sigma(W_z \cdot [h_{t-1}, x_t] + b_z)$$
$$r_t = \sigma(W_r \cdot [h_{t-1}, x_t] + b_r)$$
$$\tilde{h}_t = \tanh(W \cdot [r_t \odot h_{t-1}, x_t] + b)$$
$$h_t = (1 - z_t) \odot h_{t-1} + z_t \odot \tilde{h}_t$$

Combine CNN and GRU architectures to create the CNN-GRU model
Train The CNN-GRU model on preprocessed lung cancer dataset $\mathcal{D}$
Evaluate The trained model on a separate test dataset
Output Predicted and classified lung cancer labels for new lung cancer
End

VI. Experimental Setup

The experiments were conducted on a server equipped with an Intel i5 CPU and an NVIDIA GeForce RTX 3070 Ti GPU. Python 3.7, along with the necessary Anaconda environments, was used as the software environment for the experiments. To showcase the outstanding performance of the proposed LaCK model, we employed the hyperparameter configuration that produced the most favorable outcomes, as outlined in Table III.

TABLE III
Hyperparameter Setup for the LaCK Model

Hyperparameter	Value
DCNN Architecture	
Convolutional Layers	5
Pooling Layers	5
Filter Size	3x3
Activation Function	Adam
GRU Architecture	
GRU Units	5
Dropout Rate	0.5
Training Parameters	
Learning Rate	0.001
Batch Size	32
Number of Epochs	20

VII. Experimental Results

Figure 3 describes the numerical data distribution of lung cancer based on age. Also, Figure 4 depicts the gender classification of the possibilities of the lung cancer using the LaCK model.

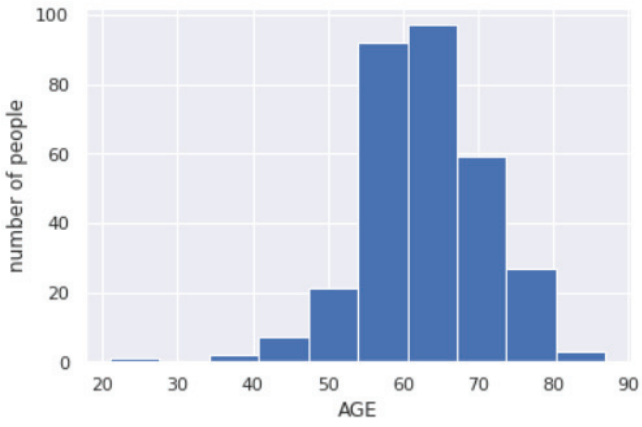

Fig. 3. Numerical Data Distribution of Lung Cancer using the LaCK Model.

Figure 12 depicts various causes of lung cancer using the LaCK model.

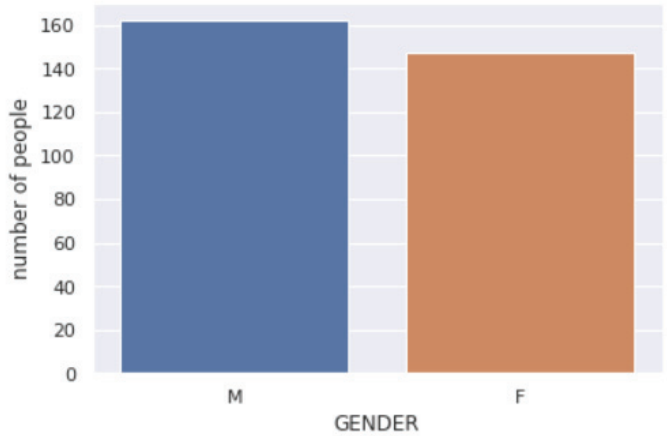

Fig. 4. The Gender Classification of the Possibilities of Lung Cancer using the LaCK Model.

Figure 5 describes the binary classification of the lung cancer using the LaCK model.

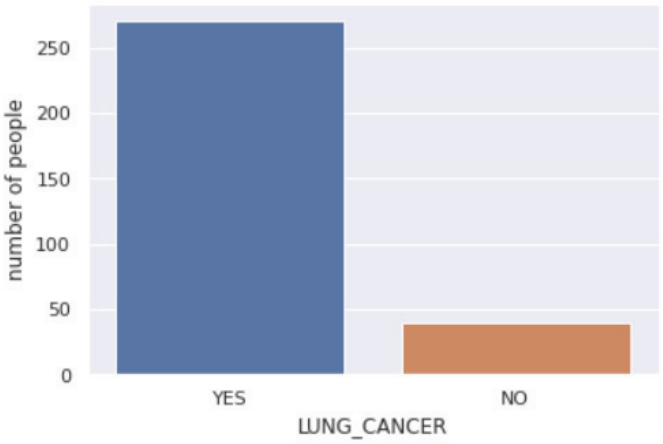

Fig. 5. Binary Classification of the Lung Cancer using the LaCK Model.

Figure 6 describes the mutual information scores of the lung cancer using the LaCK model. Figure 7 describes the confusion matrix of the lung cancer using the LaCK model.

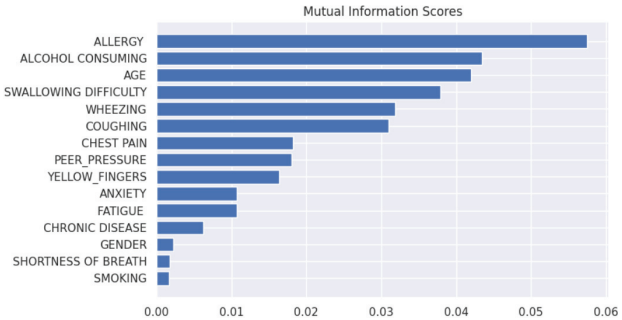

Fig. 6. Mutual Information Scores of the Lung Cancer using the LaCK Model.

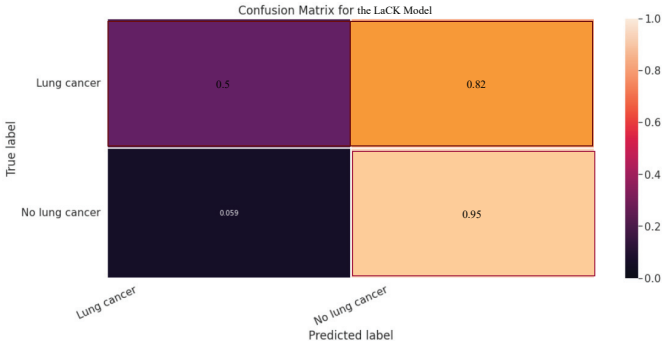

Fig. 7. Confusion Matrix of the Lung Cancer using the LaCK Model.

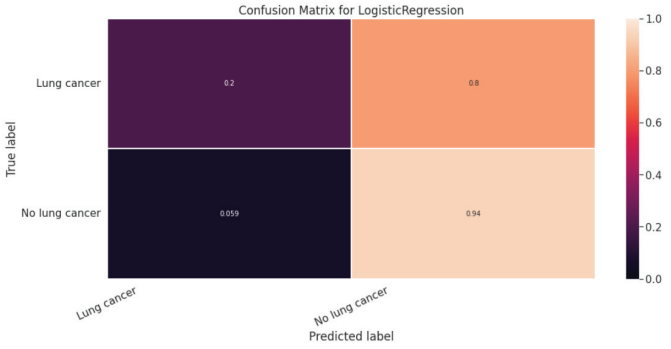

Fig. 8. Confusion Matrix of the Lung Cancer using the Logistic Regression Model.

Figure 8 describes the confusion matrix of the lung cancer using the logistic regression model [15].

Figure 9 describes the confusion matrix of the lung cancer using the SVC model [16].

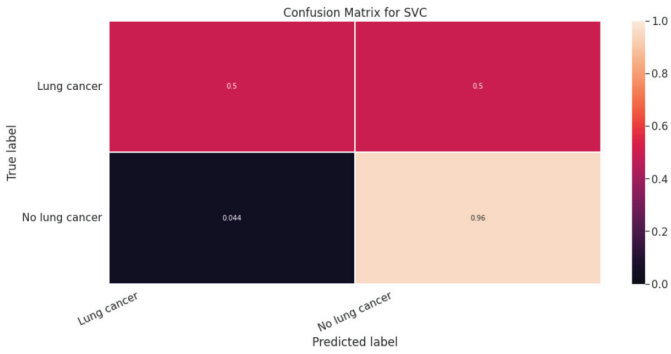

Fig. 9. Confusion Matrix of the Lung Cancer using the SVC Model.

Figure 10 describes the loss of the LaCK model.

TableIV describes the performance measures of all compared models in terms of Precision, Recall, F1-Score, and Accuracy matrices. Also, Figure 11 depicts the accuracy comparison among all the-state-of-the-art modes. From Figure 11, we observed the superiority of our proposed LaCK model.

VIII. Conclusion

Conclusion:

Fig. 10. Loss of the LaCK Model.

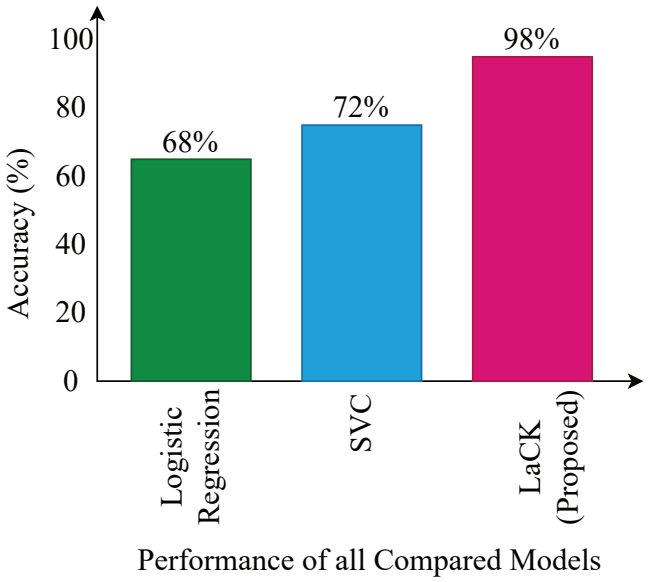

Fig. 11. Performance Comparison among all Models.

TABLE IV
PERFORMANCE METRICS

Models	Precision	Recall	F1-Score	Accuracy
Logistic Regression [15]	0.68	0.66	0.67	0.68
SVC [16]	0.71	0.72	0.721	0.72
LaCK (Proposed)	**0.956**	**0.987**	**0.975**	**0.98**

Cancer remains a pervasive threat worldwide, claiming millions of lives annually and instilling fear in countless individuals. Among its varied forms, lung cancer emerges as a significant contributor to this concerning trend. In response, our innovative research delved into lung cancer classification and detection, focusing mainly on Non-Small Cell Lung Cancer (NSCLC), which accounts for a substantial portion of cases. Through the development of lung cancer classification and detection using a convolutional neural network-based gated recurrent unit neural network model (LaCK), we aim to provide a robust solution to this pressing issue.

Employing a novel approach, we leveraged the power of five Gated Recurrent Unit Neural Networks (GRU-NN) units to achieve accurate classification. Our model was meticulously compared with logistic regression (LR) and support vector classifier (SVC) models to ascertain its efficacy. Encouragingly, the LaCK model exhibited outstanding performance, boasting a remarkable accuracy rate of approximately 98%. This notable success surpasses its counterparts' performance, showcasing our model's potential as a reliable tool for lung cancer diagnosis.

Moving forward, implementing the LaCK model in clinical settings holds promise for revolutionizing the diagnostic process for lung cancer. By providing medical professionals with a precise and automated approach to classification, our model has the potential to streamline diagnosis, expedite treatment decisions, and ultimately improve patient outcomes. Furthermore, ongoing research and refinement of the LaCK model could uncover additional opportunities for enhancing its performance and expanding its applicability in combating lung cancer and other medical challenges.

REFERENCES

[1] S. Bhatia, Y. Sinha, and L. Goel, "Lung cancer detection: a deep learning approach," in *Soft Computing for Problem Solving: SocProS 2017, Volume 2*. Springer, 2019, pp. 699–705.

[2] M. Kriegsmann, C. Haag, C.-A. Weis, G. Steinbuss, A. Warth, C. Zgorzelski, T. Muley, H. Winter, M. E. Eichhorn, F. Eichhorn *et al.*, "Deep learning for the classification of small-cell and non-small-cell lung cancer," *Cancers*, vol. 12, no. 6, p. 1604, 2020.

[3] L. Cong, W. Feng, Z. Yao, X. Zhou, and W. Xiao, "Deep learning model as a new trend in computer-aided diagnosis of tumor pathology for lung cancer," *Journal of Cancer*, vol. 11, no. 12, p. 3615, 2020.

[4] M. Geubbelmans, A.-J. Rousseau, T. Burzykowski, and D. Valkenborg, "Artificial neural networks and deep learning," *American Journal of Orthodontics and Dentofacial Orthopedics*, vol. 165, no. 2, pp. 248–251, 2024.

[5] M. F. Khatun, M. R. Ajmain, and M. Assaduzzaman, "A deep learning approach to detect and classification of lung cancer," in *2023 International Conference for Advancement in Technology (ICONAT)*. IEEE, 2023, pp. 1–6.

[6] N. Kumar, M. Sharma, V. P. Singh, C. Madan, and S. Mehandia, "An empirical study of handcrafted and dense feature extraction techniques for lung and colon cancer classification from histopathological images," *Biomedical Signal Processing and Control*, vol. 75, p. 103596, 2022.

[7] D. Hlavcheva, V. Yaloveha, A. Podorozhniak, and H. Kuchuk, "Comparison of cnns for lung biopsy images classification," in *2021 IEEE 3rd Ukraine Conference on Electrical and Computer Engineering (UKRCON)*. IEEE, 2021, pp. 1–5.

[8] W. Sun, B. Zheng, and W. Qian, "Automatic feature learning using multichannel roi based on deep structured algorithms for computerized lung cancer diagnosis," *Computers in biology and medicine*, vol. 89, pp. 530–539, 2017.

[9] A. O. de Carvalho Filho, A. C. Silva, A. C. de Paiva, R. A. Nunes, and M. Gattass, "Classification of patterns of benignity and malignancy based on ct using topology-based phylogenetic diversity index and convolutional neural network," *Pattern Recognition*, vol. 81, pp. 200–212, 2018.

[10] A. Masood, B. Sheng, P. Li, X. Hou, X. Wei, J. Qin, and D. Feng, "Computer-assisted decision support system in pulmonary cancer detection and stage classification on ct images," *Journal of biomedical informatics*, vol. 79, pp. 117–128, 2018.

[11] G. Urban, P. Tripathi, T. Alkayali, M. Mittal, F. Jalali, W. Karnes, and P. Baldi, "Deep learning localizes and identifies polyps in real time with 96% accuracy in screening colonoscopy," *Gastroenterology*, vol. 155, no. 4, pp. 1069–1078, 2018.

[12] S. Suresh and S. Mohan, "Roi-based feature learning for efficient true positive prediction using convolutional neural network for lung cancer diagnosis," *Neural Computing and Applications*, vol. 32, no. 20, pp. 15 989–16 009, 2020.

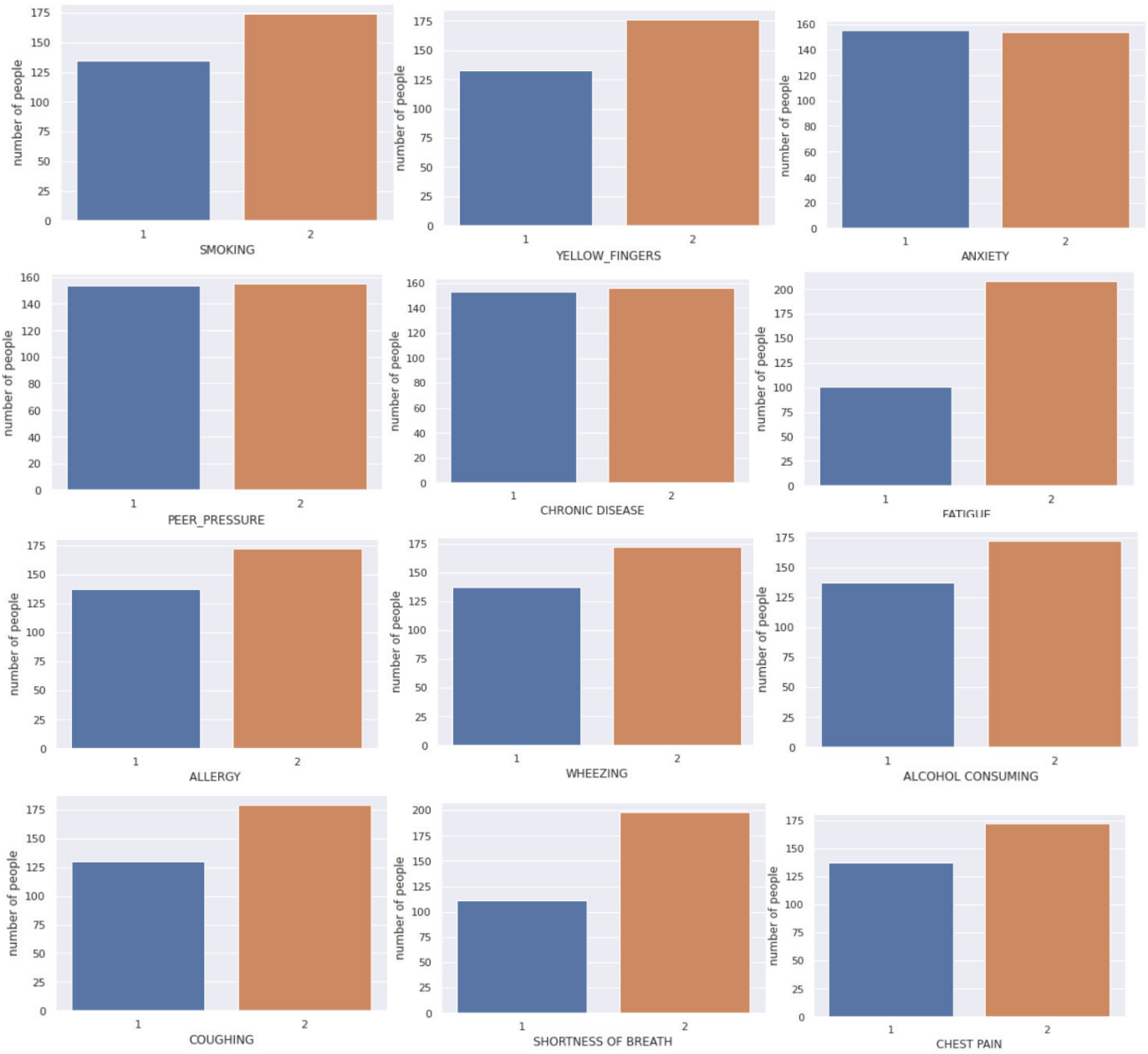

Fig. 12. Various Causes of Lung Cancer using the LaCK Model.

[13] M. Masud, G. Muhammad, M. S. Hossain, H. Alhumyani, S. S. Alshamrani, O. Cheikhrouhou, and S. Ibrahim, "Light deep model for pulmonary nodule detection from ct scan images for mobile devices," *Wireless Communications and Mobile Computing*, vol. 2020, pp. 1–8, 2020.

[14] https://www.kaggle.com/code/hasibalmuzdadid/lung-cancer-analysis-accuracy-96-4/input.

[15] M. Tirzïte, M. Bukovskis, G. Strazda, N. Jurka, and I. Taivans, "Detection of lung cancer with electronic nose and logistic regression analysis," *Journal of breath research*, vol. 13, no. 1, p. 016006, 2018.

[16] D. P. Kaucha, P. W. C. Prasad, A. Alsadoon, A. Elchouemi, and S. Sreedharan, "Early detection of lung cancer using svm classifier in biomedical image processing," in *2017 IEEE International Conference on Power, Control, Signals and Instrumentation Engineering (ICPCSI)*, 2017, pp. 3143–3148.